

Proneural gene requirements and progenitor dynamics
in sensory organ development

Sylvia Dyballa

TESI DOCTORAL UPF / 2015

DIRECTOR DE LA TESI

Dra. Cristina Pujades

BIOLOGIA DEL DESENVOLUPAMENT

DEPARTAMENT DE CIENCES EXPERIMENTALS I DE LA SALUT



4 DEVELOPMENTS

In course of this thesis I developed some methods and tools. Some of them were used for the documented research projects and others were not. However, I would like to share them with the scientific community and they will be available in the web site of the laboratory soon. They are explained in the following sections.

4.1 Implementation of a conditional gain of function approach for proneural genes

In order to study proneural requirements and potentialities of different progenitor pools, we adapted a strategy for conditional expression of the gene of interest (Gerety et al., 2013). The gene of interest is cloned into a target vector that comprises five repeats of the UAS binding sequence flanked 3-prime by a tracer (eg. *H2B-Citrine*). After insertion of the gene of interest 5'-prime of the UAS repeats induction of expression by the transcriptional activator *Gal4* leads to expression of both, gene of interest and tracer, from the bidirectional UAS repeats (see Figure 9). For conditional expression a transgenic line containing a fusion-protein of the estrogen receptor 2 (Ert2) and Gal4 under the control of the ubiquitin enhancer (*ubi::ERT2-GAL4*) was used (Gerety et al., 2013). This fusion protein is expressed ubiquitously and activation of the Ert2 receptor by tamoxifen leads to translocation of the Ert2-Gal4 to the nucleus and to target gene activation. This strategy yields a temporally controlled activation. Spatial control can be achieved in two ways; i) by expression of the Ert2-Gal4 from a tissue specific enhancer (Gerety et al., 2013) or ii) by spatially restricted activation of the Ert2-Gal4. We implemented the second strategy by using a caged version of tamoxifen called c-Cyclofen (Sinha et al., 2012). c-Cyclofen is uncaged by photoactivation with one photon 405nm light or with two-photon 750nm light (Figure 9C; (Sinha et al., 2012)). We constructed the conditional expression vectors for *neuroD*, *neuroD4* and *atoh1a*, and we have tested the *neuroD* construct (Figure 9D). In situ hybridization verified the target gene expression throughout the embryo. Preliminary results show *neuroD* positive cells as revealed by expression of the tracer in the SAG and in differentiated hair cells (Figure 9E-F). Activation of target gene expression takes about 3 hours after Ert2-Gal4 activation (Gerety et al., 2013). A strategy for assessing the cell behavior upon overexpression of the gene of interest will then be, to uncage c-Cyclofen in a

specific progenitor domain and directly live image the embryo until the tracer becomes visible and beyond. With this strategy we had planned as well to analyze combinatorial proneural gene requirements by modifying the target vector as to comprise a different tracer (eg. *H2B-EBFP*), but due to time restraints we had to abandon the project temporarily.

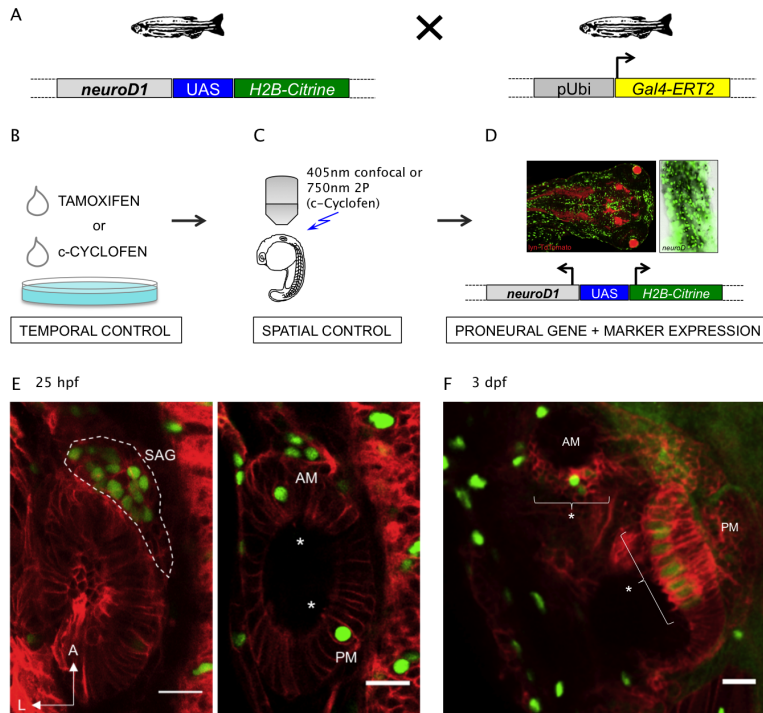


Figure 9. Conditional gain of function approach.

A) Transgenic fish with the target gene cassette are crossed with the Tg[ubi:ERT2-GAL4] line. **B)** Addition of tamoxifen to the medium allows for temporal control of target gene activation. Alternatively, c-Cyclofen can be added. **C)** Uncaging of c-Cyclofen by one- or two-photon microscopy allows for spatially restricted target gene activation. **D)** Cells that have activated the target gene can be visualized by in situ hybridization or by assessment of the tracer. **E)** *neuroD* expression was activated globally at 20 hpf with 5 μ M tamoxifen. Positive cells can be seen in the SAG (left panel), in hair cells of the posterior macula and in the neural tube (right panel). **F)** *neuroD* expression was activated by 5 μ M tamoxifen at 24 hpf overnight and embryos were imaged at 3 dpf. Positive cells can be seen in hair cells of the posterior macula but not in the supporting cell layer. E and F are single confocal planes of otic structures. The red membrane marker is lyn-TdTomato expressed from injected mRNA. Axes are indicated in E and scale bars are 10 μ m.

4.2 Evaluation of technologies suitable for long term dual color imaging of the otic vesicle

We needed an imaging setup that would allow for dual color imaging with sufficient depth penetration. Moreover it needed to be fast since we wanted to generate trackable

data. We had made some initial attempts using confocal microscopy for long-term imaging, but we discarded this setup for several reasons: first, we found that the otoliths of the otic structure led to refraction of the beam, so that we were not able to obtain sufficient resolution of the underlying structures. Second, confocal imaging being a point scanning application could not provide a sufficiently large field of view and volume for the small time interval that we needed. Third, photobleaching was elevated and in order to image for an extended time we needed an application that would show less photobleaching.

4.2.1 Imaging setups

In comparison to one photon excitation methods, two photon excitation provides a better tissue penetration due to the higher wavelengths used. Also, the two photon excitation spectra of different fluorophores overlap, so that it is possible to excite with a single wavelength two fluorophores simultaneously (Drobizhev et al., 2011; Kogure et al., 2008; Zipfel et al., 2003). Furthermore, it been demonstrated that other nonlinear methods such as second (SHG) and third harmonic generation (THG) could be obtained in biological samples without the necessity of fluorescent labeling (Olivier et al., 2010) (Witte et al., 2011). Second harmonic generation (SHG) is obtained from dense non-centrosymmetric structures such as oriented microtubule assemblies. Third harmonic generation (THG) is obtained from optical heterogeneities such as the interface between an aqueous medium and a lipidic structure (Olivier et al., 2010). We established a collaboration with the group of Pablo Loza at the Institute of Photonic Science (ICFO) to explore these methods for our purposes.

We tested:

- 1.) THG from membranes of the otic structure and we could see signal from the apical and basal membrane-water interface but not distinguish individual cells (Figure 10A). Furthermore the laser used was fixed at 1500nm, which led to decomposition of the embryo, presumably due to the higher absorption of water at this wavelength. The wavelength used in (Olivier et al., 2010) was 1200nm.
- 2.) Simultaneous excitation of red and green fluorophores at a single wavelength. We carried out tests with different fluorophores but in no case could we

establish a setup that would not lead to excessive bleaching, especially of the red fluorophore, after a short time (Figure 10B-C).

3.) Separate excitation of green and red fluorophores and also here we could not overcome the bleaching effects (Figure 10D-F).

Different fluorophores were cloned and tested for this purpose (Figure 10).

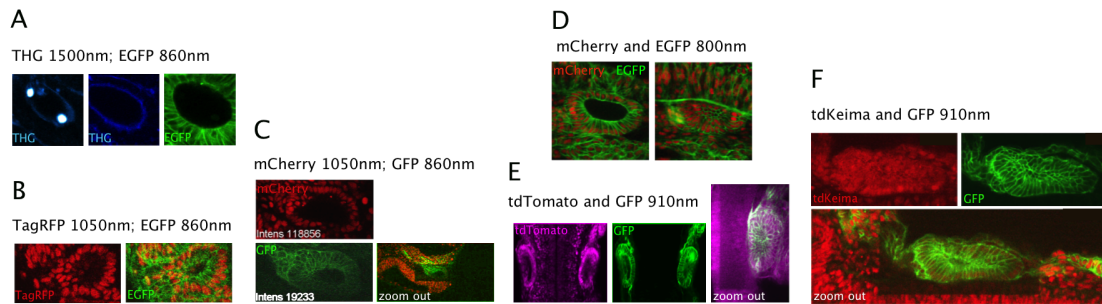


Figure 10. Nonlinear imaging of the zebrafish otic vesicle.

A) Prominent THG signal is generated from the otoliths (left). The apical and basal membranes of the otic structure can be visualized well with THG (middle), but cellular resolution cannot be obtained (compare middle and right panel). **B-C)** TagRFP and mCherry can be visualized by excitation at 1050nm. **D-F)** Simultaneous excitation of a red fluorophore (mCherry (D), tdTomato (E) and tdKeima (F)) and GFP at different wavelengths. A single stack was acquired and zooming out of the field of view highlights the elevated photobleaching (E, F). All pictures show the otic vesicle at 24 hpf.

After this, we acquired data in the facility of our collaborators from the Bioemergences platform. They provide a setup which implements separate excitation of green and red fluorophores and which is specifically adjusted for imaging of biological samples. Specifically, they provide very sensitive detectors, which allow for lowering the laser power and consequently diminishing photobleaching. Also they have implemented an incubation and temperature control system, to adjust the temperature for the specific model organism (28°C for the zebrafish). Here we could obtain some trackable data but we did not have at this moment all the transgenic lines available there, to help us in adscribing cell fates.

Finally, we turned to SPIM microscopy because it fit best our needs in the following respects: i) we could image at high speed and in a large volume, which resolved the problem of morphogenetic events and growth displacing the otic structure out of the field of view; ii) we could use the standard fluorophores in a very quick setup or even

use a triple color setup (EGFP, mCherry, Cerulean); iii) the selective plane illumination greatly diminishes photobleaching; and iv) the dual side illumination and subsequent fusion of the two views increases image quality especially in regions, like the epithelium underlying the otoliths.

The inner ear is generally a structure well suited for *in vivo* imaging. It is very superficial and comparatively small. But on the other hand it is also a very non-homogenous structure: it is spherical and contains several water lipid interfaces and additionally in the fluid filled lumen there are the two otoliths. Furthermore, it is situated adjacent to the neural tube, which is also very rich in lipids on its border. All this leads to refraction and to decreased resolution.

4.3 Image processing tools

The data we obtained from imaging with SPIM were rather large in size. A dual color single view long term imaging data set ranged typically from 300- 500GB. In a first instance we needed an efficient way to extract the data that would highlight the biological process we wanted to show (see ANNEX). For this I developed a simple script that could perform this. The focal plane of interest (FPOI) extractor script functions in the following way: The large data set is opened in FIJI as a virtual stack (FIJI on our machine can open files up to about 120GB). The user is then guided through the timesteps and confirms the plane of interest for each step. After this the different *z* planes are extracted and concatenated to generate the movie of the developmental process.

The Bioemergences platform has certain requirements as for how the imaging data has to be formatted and named: For each timestep and channel a single stack of 8bit depth is required with a specific file name, eg. **121015aX_t000_ch00.vtk.gz**. Here, 121015 is the experiment date in the format *yymmdd*, *aX* is the microscope key, *t000* is the first timepoint of the movie, *ch00* is the first channel and *vtk.gz* is the file extension (gzipped *vtk* files). In order to comply with these requirements I generated a small script that would handle these conversions and provide some additional functionalities, such as the semiautomated registration. Similar to the FPOI Extractor the user is guided to the timesteps of the movie. The user chooses a structure that is easily recognizable and

that he/she would like to be the fixpoint throughout the movie. The user then focuses this structure in z and clicks on it (x, y), which will record the location of the cursor loc (xyz). After going through the whole movie the single z-stacks for each channel are extracted, the respective transformations are performed and the files are saved with the correct filename as 8-bit .vtk files. In the same course of this registration some additional actions are performed: as we acquired SPIM data typically as 16-bit data, I introduced a user defined mapping of the 16-bit data to 8-bit that can also be set to compensate for either lighting up of transgenic lines or fluorescent bleaching. The user input that is required is displayed in Figure 11 and the **SA_registrator.ijm** script can be found on the CD and will soon be available here:

<http://www.upf.edu/devbiol/projectes/cns.html>

The FIJI plugin to save files as Bioemergences vtks was developed by Dimitri Fabrèges, and instructions for installation can be found here:

<http://bioemergences.iscpif.fr/bioemergences/resources.php>

We found that working with large data in this format is quite convenient for the simple facts that i) the data can be explored easily by iterating over subsets of the files and ii) specific strategies for image processing can be developed and tested rapidly. Another script exemplifying this usage **VTK_concatenator_processor.ijm** can also be found on the CD.

- open SPIM data as virtual stack
- define things:
 - experiment name
 - destination folder
 - if its not the first sequence: starting timestep
 - location of the fixpoint (x, y, z) in destination image stack
 - dynamic display range for each channel, eventually how to increase/decrease that range over time
- click on the fixpoint for each timestep
- wait till the process is finished
- save the image that is generated from the last timestep indicating indicating the location of the fixpoint, if successive sequences have to be processed

Figure 11. Required user inputs for the semiautomated registrator FIJI script. The user actions that are required for processing are listed (o).

5 GENERAL DISCUSSION AND OUTLOOK

The hair cell progenitor domain

In the presented research we have focused on understanding the temporal and spatial dynamics of cell fate specification and differentiation. We show that within the sensory patches the tether cells constitute the posterior poles. We have analyzed more specifically the posterior macula, since it is the territory where sensorigenesis and neurogenesis coincide.

The tether cells, as mentioned in the introduction, serve to tether the otoliths. Later in development, when more differentiated hair cells are present, there is currently no way of distinguishing later forming hair cells from the tether cells, because they share all features. Thus it was always difficult to understand the dynamics of generation of the patches. However, we knew that AM and PM develop asynchronously and asymmetrically. When analyzing the hair cell number and location of these two sensory patches at different times in development it results that the posterior macula is shifted dorsally and medially in comparison to the anterior macula, which is ventrally and more laterally located (Sapede and Pujades, 2010). Interestingly, the location of the tether cells early in development is rather symmetrical. Both pairs of tether cells are located in close proximity to the neural tube at the medial wall of the developing otic placode. This suggests, that the asymmetry of the maculae is progressively achieved during development, and is most likely a consequence of both, the location of the respective progenitor domains, and the transformation of otic topologies brought about by heterogeneous growth and cell loss from the ventral floor upon delamination of neuronal progenitors. It is tempting to speculate that the fact of having exactly two tether cells prefiguring each macula stems from a symmetric division of one tether cell precursor. From our tracking data we can say so far, that the tether cells are postmitotic from about 17hpf. It will be interesting to analyze earlier data to understand whether the tether cells are indeed sisters and how the differentiation of exactly two tether cells is achieved.

Our rationale was that the analysis of the spatiotemporal pattern of later hair cell formation in the whole organ context would lead to a better understanding of two aspects of otic development. First, we will understand the location of the prosensory domains from which hair cells are selected, and second, we will unveil the temporal

pattern of selection of these cells. To my personal surprise, the progenitor domain of the posterior macula extends over the entire ventral floor. Why is this surprising? On the one hand endogenous *atoh1a* expression is never seen in such broad territory (Millimaki et al., 2007). On the other hand, previous investigations have noted that “misexpressing *atoh1a* greatly expands the spatial domain of sensory development, typically resulting in formation of a single large macula covering the ventral/medial region of the otic vesicle”(Sweet et al., 2011). Now, considering that hair cell progenitors are distributed over this broad territory naturally, we need to reframe our understanding of the process and consider the possibility that the spatial domain of sensory development is not expanded, but rather that misexpression of *atoh1a* triggers premature differentiation of competent progenitors, which are located there. The cells in the prosensory domain are subject to Delta-Notch lateral inhibition and misexpressing *atoh1a* throughout the prosensory domain should in principle result in commitment of all these progenitors to the hair cell fate at the expense of the supporting cell fate (Haddon et al., 1998). In fact *mind bomb* mutants, defective in Notch signaling, display a phenotype reminiscent of the misexpression of *atoh1a* regarding the location and the amount of hair cells (Figure 12; (Haddon et al., 1998; Sweet et al., 2011)).

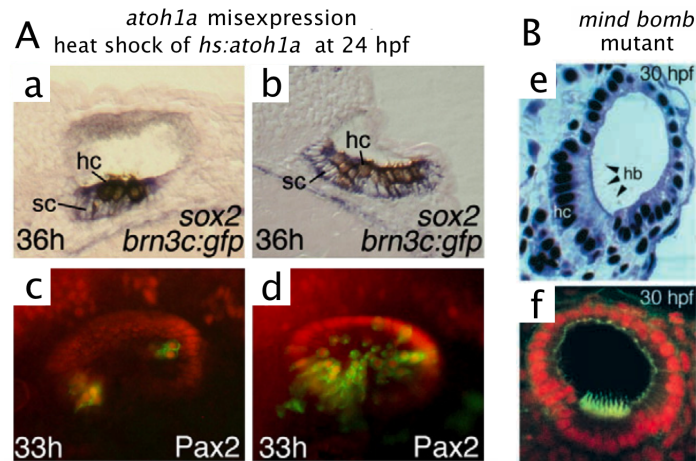


Figure 12. Hair cell phenotype upon misexpression of *atoh1a* and in the *mind bomb* mutant. **A)** Misexpression of *atoh1a* by heat shock at 24 hpf. Transverse sections showing expression of *sox2* (blue) and anti-GFP (brown) at 36 hpf in a control embryo (a) and a *hs:atoh1a* transgenic embryo (b). Expression of *brn3c:Gfp* (green) in the utricle and saccule of control (c) and in a *hs:atoh1a* transgenic embryo (d). Co-staining with anti-Pax2 in red. **B)** *mind bomb* mutant ears. Semi-thin Araldite sections stained with toluidine blue, showing the altered pattern of cell differentiation (e). Confocal image of a whole-mount specimen stained with fluorescent phalloidin (green) to reveal actin-rich hair bundles and with 7AAD (red nuclear staining) as a counterstain (f). Modified from (Sweet et al., 2011) (A) and (Haddon et al., 1998) (B).

However, the authors showed that conditional upregulation of *atoh1a* by heat shock at 24hpf results in *sox2*-positive supporting cells 12 hours later (Sweet et al., 2011). Under these conditions a functional Delta-Notch signaling might still be able to downregulate high levels of *atoh1a* and protect the supporting cell fate. Misexpression of *atoh1a* at later stages does not result in hair cell development over all the ventral floor, but rather gets confined to the territory of the sensory patches. This is likely a consequence of the expansion of the non-sensory marker *otx1* in the ventral floor (Sweet et al., 2011), (Maier and Whitfield, 2014). The details of how *atoh1* genes and *sox2* function in a genetic network are not precisely clear yet and will require further investigation.

The kinetics of hair cell differentiation

As for the question of how progenitors are selected for differentiation, we have observed, that the distribution of progenitors in the prosensory domain resembles the spatial organization of differentiated hair cells in the patch. How is the differentiation of progenitors controlled temporally? The tether cells and the nascent patches express *fgf3* and *fgf8*, which positively affect differentiation of progenitors. These signals emanating

from the differentiated cells could in principle trigger the differentiation of immediate neighbors. As PM progenitors are in rather close proximity to the AM tether cells, the question emerges why signals from these tether cells cannot trigger differentiation of these progenitors. There are different possibilities for this: i) these progenitors are in a cellular state in which FGF signals are not yet effective, thus in a non-competent state; ii) cells located in between prevent diffusible signals from arriving to these cells; and iii) there are additional mechanisms that are needed to trigger differentiation of these progenitors.

Morphological changes of hair cells upon development

In the dynamic analysis, we observed that hair cells undergo dramatic morphology changes upon differentiation. As the differentiating hair cell elevates over the epithelial layer to become incorporated to the sensory patch it extends very motile filopodia in all directions. Once it has become integrated into the upper epithelial row filopodia structures decrease. Also the progenitor leaves a basal process behind which we can observe for a while after the cell has elevated and integrated to the hair cell layer (Figure 13).

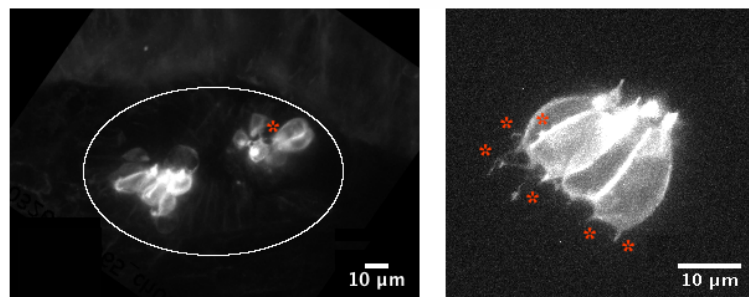


Figure 13. Morphological changes in differentiating hair cells.

Upon differentiation dynamic and transient cellular protrusions can be observed in the Tg[Brn3c:GFP] line, that labels the membrane of differentiated hair cells. Asterisks indicate cellular these protrusions in hair cells of the PM (left) and the AM (right). The otic vesicle is outlined in (left), and both are dorsolateral views with anterior to the left and dorsal to the top.

We do not know at the moment if these cellular processes are indeed transient structures that the progenitors exhibit only upon differentiation as we observe them only once the membrane marker Brn3C:GFP starts to be expressed. Another open question is whether they can have functional relevance in i) finding and joining the already differentiated hair cells of the patch, ii) signaling to neighboring cells to differentiate, or iii) in

establishing contact with the innervating axon, in the case of the basal process. Finally, we still need to understand whether these morphology changes are specific of hair cells or if all cells of the otic epithelium exhibit these phenotypes.

Delamination domain and the Statoacoustic Ganglion (SAG) rudiment

The role of *neurog1* in defining cranial sensory ganglion precursors is very well established (Figure 14; (Andermann et al., 2002)). The SAG is initially fused with neuroblasts of the anterior lateral line ganglion (ALLg) and the general opinion was i) that all components of the SAG derive from delamination from the otic vesicle, and ii) that the neuroblast population that is found at placodal stages anterior to the otic vesicle belongs exclusively to the ALLg, implying that otic neurogenesis needs the placodal/vesicular infrastructure.

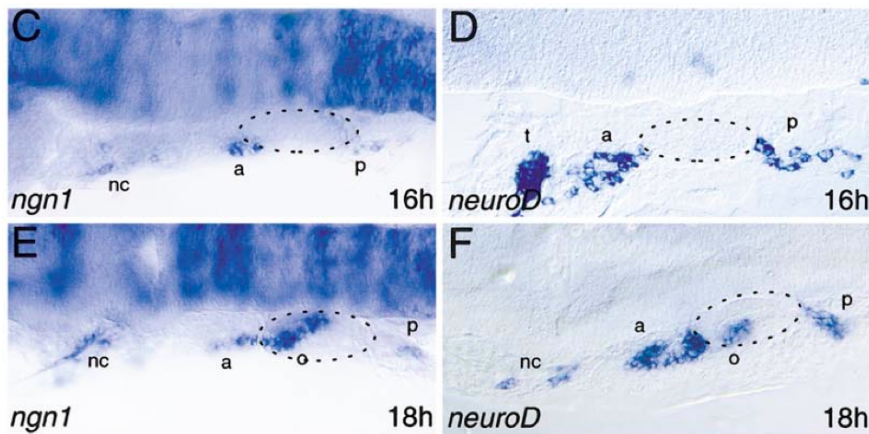


Figure 14. *neurog1* and *neuroD* expression in developing zebrafish cranial ganglia. *neurog1* (*ngn1*) and *neuroD* expression reveals the positions of the dorsolateral placodes. Panels show lateral views of zebrafish heads just posterior to the eye with anterior to the left and dorsal to the top. Neurogenic dorsolateral placodes form at the edges of the otic placode/ vesicle outlined with a dashed line. a, anterior lateral line placode area; nc, neural crest; o, octaval/statoacoustic ganglion precursors; p, posterior lateral line placode/ganglion. Adapted from (Andermann et al., 2002).

Recently this view was challenged by research showing that neuronal competence is readily provided upon OEPD specification by *Foxi1* (Hans et al., 2013). Likewise, in chick it had been shown before that *Sox3* is expressed in the OEPD where it establishes the neurosensory domain (Abelló et al., 2010). In our work, we observe that neuroblasts contributing to the ALLg as well as to the SAG are located anteriorly to the forming

otic placode. Upon placode formation otic precursors acquire an ordered arrangement and a columnar shape. This ordered arrangement starts first in the otic cell population adjacent to the neural tube, and a bit later also the lateral domain of the forming otic placode becomes arranged in this ordered fashion. While the placode undergoes these morphological changes neuroblasts located anteriorly of the structure begin to differentiate. We verify by lineage tracing that these cells are truly otic and denominate this population of cells the early SAG neuroblasts or SAG rudiment. We also show that these neurons are the first to contact the neural tube upon differentiation where they send projections into the developing hindbrain to establish the circuit (Zecca et al., 2015), and that they already innervate their peripheral targets, the tether cells of the AM and PM. However, this population of neuroblasts is small compared to the bulk of cells that will delaminate from the otic epithelium. As the placode/ vesicle forms, neuroblasts continue to be specified at the antero-lateral domain. Within only about one hour this delamination domain from which cells exit the epithelium expands to the postero-medial aspect. During the consecutive hours of development many cells undergo apical constriction, and Epithelial to Mesenchymal Transition (EMT) to delaminate from this domain. It is currently not clear what are the cellular mechanisms that drive delamination from the otic placode (Lassiter et al., 2014) (Breau and Schneider-Maunoury, 2014). Expression of *neuroD* in these neuroblasts appears to be of mayor importance for delamination (Liu et al., 2012b), and FGF signaling likely mediates cytoskeleton remodeling as a consequence of specification similar to the one described in otic invagination (Sai and Ladher, 2008) (Harding and Nechiporuk, 2012) (Gonzalez and Medici, 2014). Other signaling inputs such as Wnt, Bmp, Shh and signals from the extracellular matrix have been implicated in the process of delamination, however, their role in otic delamination remains to be investigated. The zebrafish inner ear might be a good model to study the mechanisms behind these cell morphology changes and this is likely to be beneficial as the process of EMT is important in cancer metastasis. We have shown that automatic single cell segmentation is feasible and a systematic analysis of cell morphology changes in manipulated embryos will yield deeper insights in the mechanistic properties of the system.

Neuronal identities and temporal requirements

The AM and PM of the zebrafish inner ear constitute two sensory modalities, as the AM is involved in vestibular function, while the PM seems to be involved in both functions, audition and vestibular (Haddon and Lewis, 1996; Whitfield et al., 2002). This implicates that sensory inputs from these two sensory patches need to be integrated differentially at the central level. Previous research from our group showed that the SAG is segregated into two main populations, which innervate specifically each macula and send segregated central projections into the hindbrain (Sapede and Pujades, 2010). Furthermore, we have recently shown that the time and place of differentiation of cranial ganglia prefigures the somatotopy of central projections in general (Zecca et al., 2015).

This leads to the question of how auditory versus vestibular neurons are specified. In mice *gata3* is expressed in the otic epithelium, most notably in the sensory epithelia, and in auditory neuroblasts. Initially all neuroblasts express *neuroD*, but neuroblasts of the spiral ganglion lose *neuroD* expression and maintain *gata3* expression. In contrast, vestibular neuroblasts do not express *gata3* but maintain *neuroD* expression (Lawoko-Kerali et al., 2004). It has been suggested that *gata3* would be involved in axon pathfinding, on the one hand because *gata3* is expressed in the developing cochlea and in innervating afferent auditory neurons of the CVG, and on the other hand because it is also expressed in efferent neurons that innervate the vestibular or the auditory sensory epithelia (Lawoko-Kerali et al., 2001) (Karis et al., 2001). Functional experiments have confirmed this notion and upon loss of *gata3* cochlear wiring is severely disrupted (Appler et al., 2013).

In chicken *gata3* is expressed in the prosensory domains but not in delaminating neuroblasts. Only after auditory neuroblasts have undergone the terminal mitosis *gata3* is upregulated in these cells, but not in vestibular neurons (Jones and Warchol, 2009). Finally, in zebrafish *gata3* is expressed in the otic epithelium and also in a subset of the neuroblasts in the ganglion at 32hpf (Figure 15; (Sapede et al., 2012)). However, no specific molecular signature has been defined for the different SAG cell populations. For what is known, most of the neuroblasts share the same gene expression profile.

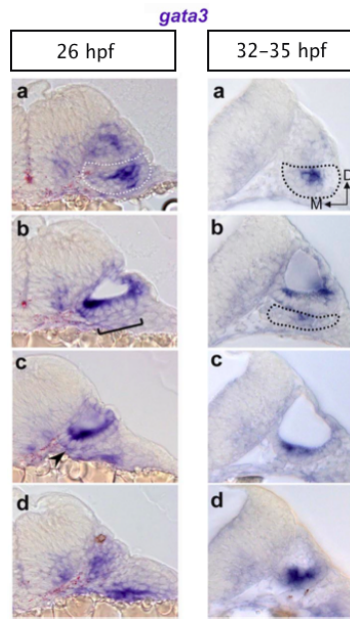


Figure 15. *Gata3* expression in the zebrafish inner ear.

Transverse sections from anterior (a) to posterior (d) throughout the otic vesicle of 26 hpf (left column) and 32- 35 hpf (right column) embryos hybridized with *gata3*. At 26 hpf, the forming SAG is found only in the most anterior section (a, dotted lines). Brackets in b sections indicate the broader delaminating zone. Arrowheads in c indicate the posterior part of the neurogenic domain. At 32-35 hpf the SAG extends in the two first sections (a, b; dotted lines). Modified from (Sapede and Pujades, 2010).

It would be interesting to compare this expression directly to our cell-tracking data to understand in which neuronal subpopulation *gata3* is expressed here. The expression of *gata3* in the otic epithelium might correspond to the progenitor domain of PM hair cells. In fact, one of our future plans is to combine high-resolution image data of fluorescent in situ hybridization with the results obtained from the cell-tracking analysis (see below).

The mouse cochlea displays a tonotopic organization but *gata3* is expressed in virtually all the cells of the spiral ganglion. So how do these neurons find their correct target, both in the cochlea and in the cochlear nuclei of the brainstem? One possibility is that the circuit is established only once sensory hair cells have differentiated, in an activity dependent manner. It is very clear that maintenance of the circuit is strongly dependent on activity as the central targets die upon loss of peripheral targets and recently it was suggested that there is a critical period for survival, differentiation and dendritic development (Elliott et al., 2015; Levi-montalcini, 1949).

However, activity seems not to be required for initial circuit assembly, as spiral ganglion neurons can readily innervate their peripheral and central targets while these are still immature (Koundakjian et al., 2007), (Fritzscht et al., 2005). Koundakjian et. al used a *neurog1-Cre* line and induced recombination in epithelial neuroblasts at different times of development. This genetic lineage tracing allowed for analysis of how birthdate correlates with identity. Cre-recombination, as early as E8.5, resulted in strong labeling

of the vestibular ganglion with little or no labeling in the spiral ganglion. Later Cre-recombination (E12.5) produced labeled cells in the spiral ganglion and only few in the vestibular ganglion. Cre-recombination at E13.5 gave few or no cells labeled in either ganglion. Accordingly at the central level, projections from different neuronal populations are located at stereotypical locations in the yet immature cochlea-vestibular nucleus. Furthermore, Cre-recombination at different times could reveal a bias of neuroblasts to innervate specific domains of the cochlea (Figure 16; (Koundakjian et al., 2007)).

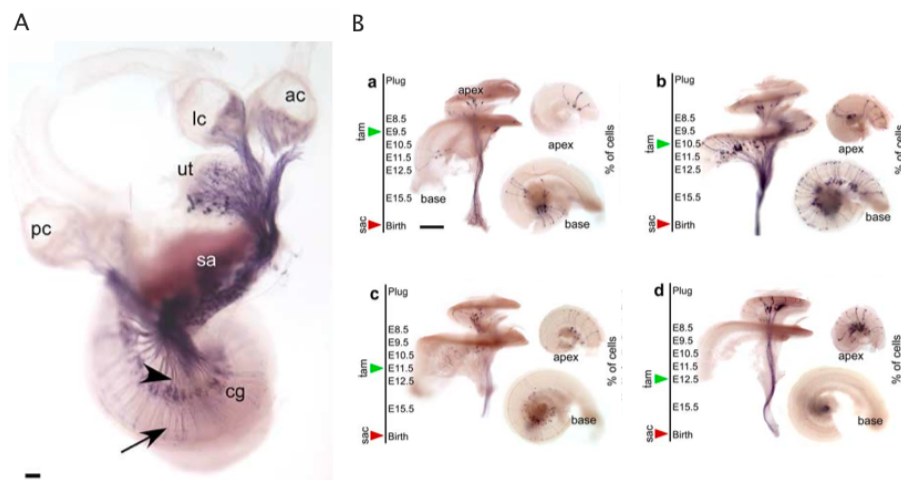


Figure 16. Genetic tracing of neuroblasts derivatives and their innervation pattern in mouse cochleas.

A) Cochlear ganglion neurons (cg) are labeled along their entire length, including peripheral (arrow) and central (arrowhead) processes. Vestibular projections are also labeled and can be seen innervating the anterior (ac), lateral (lc), and posterior (pc) cristae, as well as the utricle (ut) and saccule (sa). PLAP-stained inner ear dissected from a *Ngn1-CreER^{T2}; Z/AP* animal that received 1 mg of tamoxifen at E10.5 and was collected on P0. Scale bar, 100 μ m. **B)** Activation of Cre activity at E9.5 sparsely labeled neurons in the mid-basal region (a). One day later, labeling was extensive throughout the base and in the middle of the cochlea, with little in the apex (b). Tamoxifen treatment on E11.5 predominantly labeled neurons in the middle turn (c), whereas treatment on E12.5 exclusively labeled neurons in the apex (d). P0 cochleas dissected from *Ngn1-CreER^{T2}; Z/AP* animals that were given 0.5 mg of tamoxifen (tam) at the times indicated, killed at birth (sac), and stained for PLAP activity. Each cochlea was cut in half and imaged from the basal surface to best visualize the distribution of labeled neurons in the apex and base. Scale bar, 500 μ m. Modified from (Koundakjian et al., 2007).

The authors conclude that, “although it is tempting to speculate that tonotopic maps arise passively with early arriving axons simply projecting to the dorsal-most regions of the cochlear nucleus, a more likely model is that molecular differences in axons from different regions of the cochlea guide topographic map formation”. Candidates for such molecular determinants in mammals are Trk receptors, which are differentially

expressed along the cochlea (Fariñas et al., 2001), or Eph receptors, which have been already implicated in regulating tonotopical sensory maps (Siddiqui and Cramer, 2005). Apart from the stereotyped wiring decisions that follow a temporal scheme, also the topology of neuroblast (cell body) allocation is temporally controlled. The trigeminal ganglion (TGg) is responsible for the detection of a range of stimuli such as chemical, mechanical and thermal stimuli. The generation of specific identities is restricted to different times of development: photoconversion analysis paired with assessment of identity-specific molecular markers revealed that chemosensitive neurons form exclusively from early born neurons, while mechanosensitive neurons can be generated from both, early and late born neurons (Caron et al., 2008). In the TGg only the early neurogenesis is dependent on *neurog1*. Late neurogenesis can occur after 24hpf without *neurog1* inputs, but upon abrogation of early neurogenesis, chemosensitive neurons never form (Caron, 2013). This can on the one hand reflect the temporal requirements, but it may also point to specific molecular requirements such as *neurog1* for this neuronal subtype. Such molecular requirements and temporal dependencies have also been studied in the olfactory bulb. *Neurog1* and *neuroD4* are both expressed during early morphogenesis, but while expression of *neurog1* vanishes after a while, *neuroD4* persists during late neurogenesis. The abrogation of *neurog1* leads to a delay of *neuroD4* expression. As a consequence only few early otic neurons are specified which also fail to display some early otic neuron markers. These were only two examples highlighting the temporal requirements in cell fate specification and it is generally well accepted by now that the time of differentiation has an influence on cellular identity (Cepko, 2014) (Guillemot, 2007). Our results in otic neurogenesis reveal a very strong correlation of spatial (AP-axis) and temporal parameters between the positions of neuroblasts in the otic epithelium versus their positions in the SAG. The spatial correlation in both axes (AP and ML) is quite plausible when considering the kinetics of delamination. After rapid establishment of the delamination domain cells exit the epithelium from any place within this territory for an extended period of time. Newly delaminated cells seem to search the contact to the already-delaminated neuroblasts, which are positioned medially. It is quite straight forward to imagine how a medio-lateral arrangement can be generated for example on the basis of differential cell adhesion or attractive cues from the more differentiated towards the recently

delaminated neuroblasts. As described before, FGF and Eph/Ephrin signaling are good candidates to keep the arrangement that first cells to delaminate will be always more medially located within the SAG than late delaminated neuroblasts. In any case, our results highlight the importance of timing in establishment of the SAG organization as well as in the establishment of the topographical organization of the central projections of different cranial sensory ganglia.

In how far might our findings be recapitulated in other models? In chick and mice it appears that vestibular neuroblasts are born before auditory ones (Bell et al., 2008; Koundakjian et al., 2007), while in our system posterior and anterior neuroblasts delaminate concomitantly from the otic epithelium. Evolution might have transformed the topologies of the different domains to account for generation of an evermore-sophisticated auditory structure. From an evolutionary prospective the cochlea is commonly viewed as an outgrowth of the saccule and the generation of this endorgan should be in part a result of topological changes of the progenitor domains. Naturally these alterations can impact the temporal sequence of events; in fact in amniotes not the maculae but the cristae are the first to display differentiated hair cells. In any case, the zebrafish contains the two basic sensory modalities and the knowledge of where progenitors are located and how they give rise to the different sensory elements might help in investigating the question of what defines their identity.

Proneural gene requirements

We have investigated the proneural gene requirements in the different progenitor pools. We show that in the postero-medial aspect of the otic epithelium, progenitor domains for hair cells and neurons are in close proximity and might partially overlap. Upon downregulation of *neurogl* no neuroblasts are produced. Instead this inhibition results in the generation of supernumerary hair cells in the PM. The notion that hair cells and neurons are related clonally has come from different experiments (see INTRODUCTION and below). Genetic tracing in mice embryos could show that i) *NeuroD* is normally expressed in some hair cells of the cochlea and upon inhibition of *neurogl* more *neuroD* positive hair cells are present, and ii) *atoh1* is normally expressed in some neurons of the CVG (Figure 17;(Matei et al., 2005)).

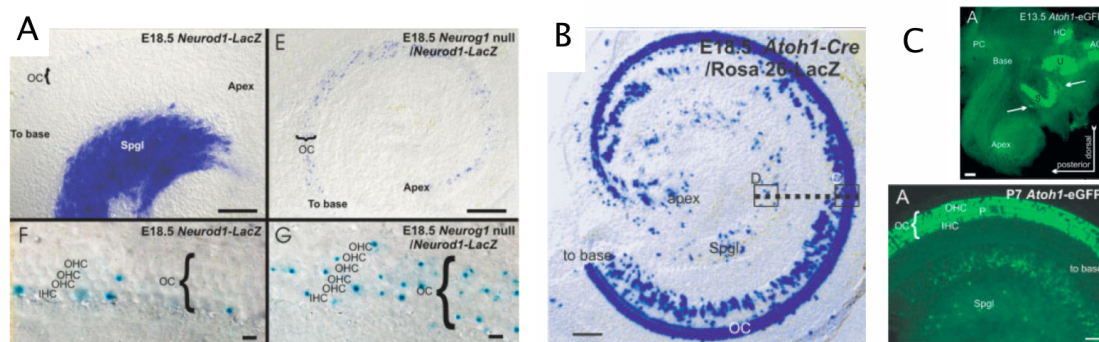


Figure 17. *NeuroD* and *Atoh1* expression in mouse spiral ganglion and cochlea.

A) *Neurod1-LacZ* expression at E18.5 in a *Neurod1-LacZ* heterozygote wild type and *Neurog1* null littermate. At E18.5, spiral neurons are strongly labeled for *Neurod1* in the wild-type ear (top left). In contrast to the very faint labeling of the wild-type organ of Corti (bottom left), the *Neurog1* null ear (bottom right) shows profound *Neurod1-LacZ* staining in many hair cells. Note the absence of spiral ganglion neurons in *Neurog1* null mice (compare top left and top right) and the multiple rows of outer hair cells in the apex of the mutant cochlea (compare bottom left and bottom right). **B)** Expression of *Atoh1-Cre* as revealed with a Rosa 26 line is shown in a flat mounted cochlea of an E18.5 embryo ear. Hair cells are most profoundly positive for the β -galactosidase reaction product. However, additional cells in the cochlea are also positive. Note that *Atoh1-Cre* staining can be shown in some spiral ganglion neurons. **C)** Expression of *Atoh1-eGFP* in hair cells and sensory neurons of E13.5 (top) and juveniles (bottom) is shown. At E13.5, *Atoh1-eGFP* shows a profound signal in the vestibular sensory epithelia and in some delaminating cells (arrows in top). IHC, inner hair cell; OHC, outer hair cell; OC, organ of Corti; Spgl, spiral ganglion. Scale bars 100 μ m. Modified from (Matei et al., 2005).

Knockdown of *neurog1* in the mouse inner ear results in smaller ears with no sensory neurons that comprise smaller sensory epithelia with fewer differentiated hair cells (Ma et al., 2000). Accordingly, our results show that upon downregulation of *neurog1*, either by morpholino injection or by hypomorphic mutation, the zebrafish inner ear is devoid of sensory neurons. The hair cell fate is unaffected in the AM but non-specified neuronal progenitors switch to the hair cell fate such that the PM incorporates supernumerary hair cells. Furthermore, the inner ear is not smaller but bigger at 24hpf due to the fact that neurons are not specified and therefore they do not delaminate and stay integrated in the otic epithelium. The increased size of the vesicle results in an enlarged progenitor domain from which more hair cells can be recruited. We also show that the proliferative behavior is not different in control and *neurog1* depleted fish, which further supports this hypothesis. As regarding the question of why the increase of PM hair cells is moderate (only about double as many as in the control) compared to the number of neuroblasts that presumably exhibit the potential to switch fate, there are different possibilities: i) we see no difference in the spatial pattern of hair cell

incorporation in these fish, and this might reflect that self-organizing mechanisms which control the differentiation of progenitors work equally well even if the domain is expanded. In this respect *neurog1* would merely provide a competence; ii) *neurog1* alone may not be sufficient and additional regional cues are required for differentiation. Hedgehog from the notochord would be a candidate in this case; and iii) cell intrinsic factors are required for differentiation, which not all of the non-delaminated neuroblasts contain. *NeuroD* is a candidate since it has been shown to play a role in hair cell development.

In the zebrafish lateral line *neuroD* is required for hair cell differentiation within the neuromasts. Here *atoh1* overexpression can induce *neuroD*, and *neuroD* can rescue the phenotypes upon inhibition *atoh1*. This suggests that in the lateral line *neuroD* is a target of *atoh1* (Sarrazin et al., 2006). In fact, while in the peripheral nervous system *neuroD* is best described as a downstream target of *neurog1*, at the central level *atoh1* positive granule cell precursors also express *neuroD* (Kani et al., 2010).

Regarding the role of *neuroD* in otic development, functional experiments have suggested, that in delaminated neuroblasts the expression of *atoh1* needs to be repressed and that *neuroD* is responsible for it. Upon *neuroD* knockdown in mice the authors detected agglomerates of sensory hair cells within the statoacoustic ganglion. Furthermore, they detected defects in the organization of the organ of Corti, in which premature differentiation of hair cell precursors led to generation of more rows of inner hair cells and fewer rows of outer hair cells (Figure 18; (Jahan et al., 2010)).

These findings in other systems led us to address the role of *neuroD* in the zebrafish inner ear. Upon inhibition of *neuroD* we observed a decrease in the number of hair cells specifically in the posterior macula, suggesting that *neuroD* might have a positive role on hair cell development in this sensory patch. In *neurog1*-MO and *neurog1*-mutant embryos no *neuroD* expression was detected in the epithelium early in development, as expected, because *neuroD* is a known downstream target of *neurog1* in the ear. However, later in development these embryos display *neuroD* specifically in the PM, suggesting that the late *neuroD* expression wave is independent of *neurog1*. We could never observe transcript or protein of *neuroD* in differentiated hair cells, but we show by rescue experiments in *neurog1*-depleted embryos, that *neuroD* is required for generation of hair cells from the bipotent progenitors. We propose that *neuroD* is

differentially regulated in different progenitor pools, being under the control of *neurogl* in the neuroblast pool and under the control of *atoh1* later in the bipotent progenitor pool. It will be interesting to investigate the potentialities of *neuroD* in these different pools directly by conditional activation (see DEVELOPMENTS). Another approach could be to downregulate *neurogl* in the Tg[neuroD:GFP] line and directly image the dynamic behavior of the neuroD-positive pool.

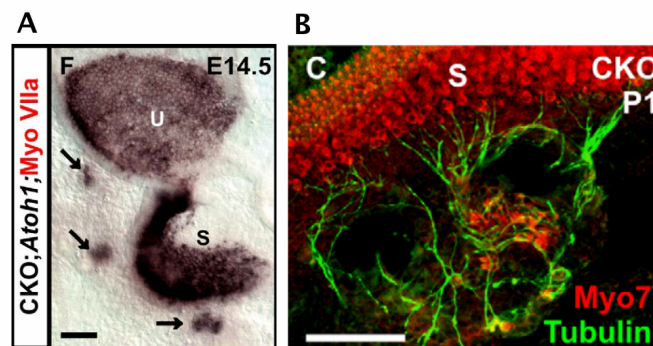


Figure 18. Absence of *Neurod1* results in formation of MyoVIIa positive ectopic hair cells in inner ear ganglia in mice.

A) Persistent *Atoh1* expression in remaining ganglia relates to transformation of ganglionic cells into hair cells in *Neurod1* mutants. In situ hybridization of *Atoh1* appears in clusters of cells in CKO mutants near the utricle and saccule (arrows). B) Whole mount Immunofluorescence labeling with Myo VIIa marks the hair cells in the vestibular epithelia and Myo VIIa positive cells are also found outside the sensory epithelia interspersed among the remaining vestibular ganglia near the utricle and the saccule from E14.5 until adulthood. These Myo VIIa positive cells are often grouped around intraganglionic vesicles. Immunofluorescence labeling with anti- β -tubulin shows innervation of these Myo VIIa positive cells. Scale bars 100 μ m; U, utricle; S, saccule. Modified from (Jahan et al., 2010).

The bipotent progenitor

By single cell photoconversion we crudely mapped the location of progenitors with different potentialities and demonstrated the existence of a single cell that gives rise to both hair cells and neurons. From our lineage studies it emerged that i) the progenitors of the first hair cells are postmitotic at 24hpf and that the vast majority of neuroblasts divides symmetrically to give rise to two delaminating daughters. Only in few cases in cells located at the border of the delamination domain we detect delamination of one daughter but not of the other one. This of course has little implication, as we do not know if these cells delaminate later on in development. When analyzing the sensory domain from 24hpf onwards, we never observe delamination from this region but few

events could be detected laterally adjacent to the sensory domain. Experimentally it has proven difficult to analyze both progenitor pools in one data set due to the morphology of the structure and the spatial distribution of these pools within. So since we can never detect a cell giving rise to a neuroblast and to a hair cell in the tracking data, this leads to different conclusions: i) the generation of the hair cell and neuronal fates from one cell happens as a general mechanism in few cells later in development and might involve asymmetric division; ii) the generation of the different fates from a single progenitor is sequential and we cannot get examples in our datasets; or iii) the generation of both fates is a result of imprecision in gene expression and happens accidentally, however cells able to switch fates are present in the epithelium in case of need.

Why is there so much interest in a common progenitor? Previous research has made it very clear that proneural genes co-regulate each other in the specification of different fates. In the CNS and also in the retina this commonly involves the sequential generation of different fates from multipotent progenitors whose potential gets restricted in time dependent manner. Vertebrates have adapted proneural gene regulation for peripheral neurogenesis and it is not clear to what extent peripheral neurogenesis resembles neurogenesis in the brain; and to begin with the precise mechanisms are neither clear for the latter. One could argue that understanding proneural gene function in fate specification has therapeutic implications, even if we can readily regenerate hair cells from iPS cells (Aida Costa et al.). Anyhow, a better understanding of the molecular mechanism will probably be beneficial for the development of regenerative strategies. Finally, while we show that the progenitor domains of hair cells and neurons are segregated in the early zebrafish inner ear, this does not necessarily mean that the same is true for chick and mice, since we already know that sensorigenesis happens once neurogenesis has almost ended.

So what can we learn from the zebrafish? And what does a spatiotemporal analysis of the development of the inner ear bring? I think the description is of value for the scientific community in different respects. First, the knowledge of where progenitors are located and how they differentiate allows for a better interpretation of phenotypes as described above. Second, it will be a good reference when designing experimental

strategies that aim to conditionally manipulate a given progenitor pool. Third, it is possible to map fluorescent in situ data onto the tracking data. Recently a framework (VIBE-Z) for generating a gene atlas for the 72 hpf zebrafish brain has been presented (Figure 19; (Liu et al., 2012a)). It is feasible to create a comparable atlas for the inner ear (personal communication with O. Ronneberger) and combine it with tracking data. For this it will be surely necessary to generate more tracking data to account for interindividual differences. Finally, instead of -or additionally to- using in situ hybridization data, quantitative RT-PCR data could be used to create or complement such atlas. This has been nicely demonstrated for the mouse otocyst. The authors dissolved GFP-labeled otocyst cells and FACS sorted them to conduct cell expression profiling on each single cell. By subsequent cluster, principle component and network analysis these individual cells were grouped and their spatial relationships were reconstructed by bioinformatic modeling. Despite the small number of cells analyzed (382 with otocyst and early ganglion included) the approach could recapitulate topological relationships of known gene expression domains. Importantly, this approach is sensitive to different expression levels, the importance of which is well established (McCarroll et al., 2012), (Pan et al., 2012). Furthermore, it can reveal new lineage or progenitor specific markers ((Cai et al., 2015)).

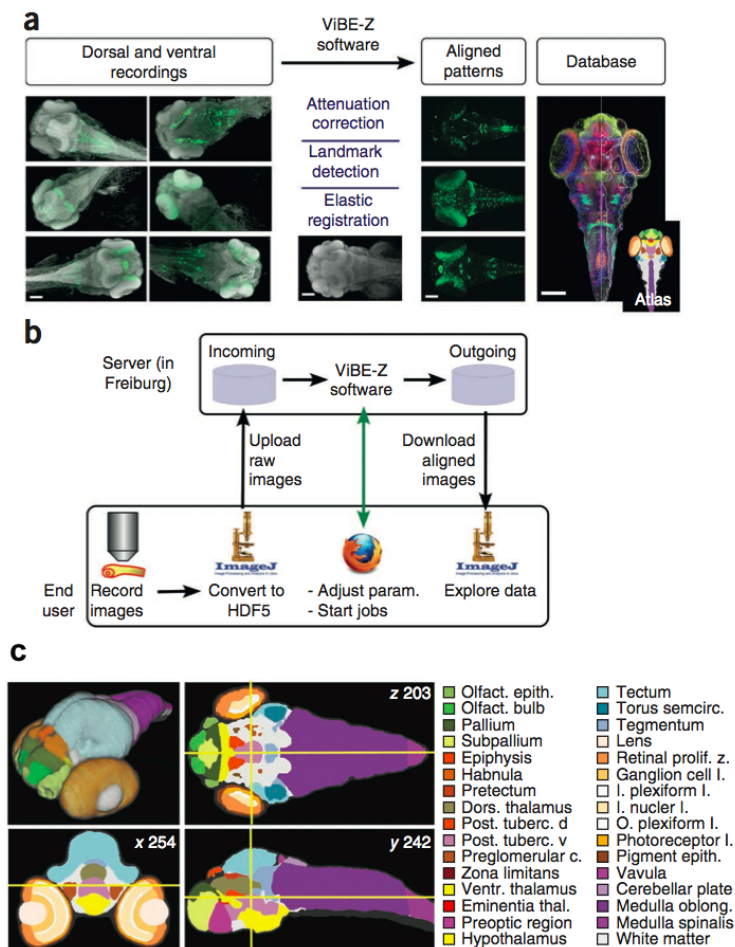


Figure 19. The Virtual Brain Explorer for Zebrafish (ViBE-Z).

(a) ViBE-Z overview. Input: different individuals recorded from two viewing directions (dorsal and ventral). Each recording consists of two channels: gray, nuclear stain; green, gene expression pattern. Output: aligned gene expression patterns for the ViBE-Z database and atlas. All scale bars are 100 μ m. (b) ViBE-Z usage: the software will be provided to other scientists through a web-based interface. (c) Anatomical segmentation of the reference zebrafish larva. Clockwise from top left: surface rendering, transversal section, lateral section, frontal section. Planes indicated by numbers, yellow lines. Abbreviations: c, complex; d, dorsal; i, inner; l, layer; o, outer; post, posterior; v, ventral; z, zone. Modified from (Liu et al., 2012a).

6 ANNEX

6.1 Study of the spatiotemporal establishment of the establishment of cranial sensory ganglia central projections and their topographical organization

Zecca, A, Dyballa, S, Bradley, R, Pujades, C. The order and place of neuronal differentiation establish the topography of sensory projections and the entry points within the hindbrain,

J Neuroscience 35(19):7475-86. doi: 10.1523/JNEUROSCI.3743-14, 2015

Zecca A, Dyballa S, Voltes A, Bradley R, Pujades C. [The Order and Place of Neuronal Differentiation Establish the Topography of Sensory Projections and the Entry Points within the Hindbrain.](#) J Neurosci. 2015 May 13;35(19):7475-86. doi: 10.1523/JNEUROSCI.3743-14.2015.

7 BIBLIOGRAPHY

- Abbas, L., Whitfield, T. T., Perry, S. F. and Ekker, M.** (2010). The zebrafish inner ear. *Fish Physiology:*
- Abelló, G. and Alsina, B.** (2007). Establishment of a proneural field in the inner ear. *Int. J. Dev. Biol.* **51**, 483–493.
- Abelló, G., Khatri, S., Radosevic, M., Scotting, P. J., Giráldez, F. and Alsina, B.** (2010). Independent regulation of Sox3 and Lmx1b by FGF and BMP signaling influences the neurogenic and non-neurogenic domains in the chick otic placode. *Developmental Biology* **339**, 166–178.
- Aida Costa, Luis Sanchez-Guardado, Juniat, S., Gale, J. E., Daudet, N. and Domingos Henrique** Generation of sensory hair cells by genetic programming with a combination of transcription factors. *Development* **142**, 1948–1959.
- Alsina, B., Abelló, G., Ulloa, E., Henrique, D., Pujades, C. and Giraldez, F.** (2004). FGF signaling is required for determination of otic neuroblasts in the chick embryo. *Developmental Biology* **267**, 119–134.
- Alsina, B., Giraldez, F. and Pujades, C.** (2009). Patterning and cell fate in ear development. *Int. J. Dev. Biol.* **53**, 1503–1513.
- Andermann, P., Ungos, J. and Raible, D. W.** (2002). Neurogenin1 Defines Zebrafish Cranial Sensory Ganglia Precursors. *Developmental Biology* **251**, 45–58.
- Appler, J. M., Lu, C. C., Druckenbrod, N. R., Yu, W. M., Koundakjian, E. J. and Goodrich, L. V.** (2013). Gata3 Is a Critical Regulator of Cochlear Wiring. *Journal of Neuroscience* **33**, 3679–3691.
- Arnold, J. S., Braunstein, E. M., Ohyama, T., Groves, A. K., Adams, J. C., Brown, M. C. and Morrow, B. E.** (2006). Tissue-specific roles of Tbx1 in the development of the outer, middle and inner ear, defective in 22q11DS patients. *Hum. Mol. Genet.* **15**, 1629–1639.
- Basch, M. L., Brown, R. M., Jen, H.-I. and Groves, A. K.** (2015). Where hearing starts: the development of the mammalian cochlea. *J. Anat.*
- Bell, D., Streit, A., Gorospe, I., Varela-Nieto, I., Alsina, B. and Giraldez, F.** (2008). Spatial and temporal segregation of auditory and vestibular neurons in the otic placode. *Developmental Biology* **322**, 109–120.
- Bermingham, N. A.** (1999). Math1: An Essential Gene for the Generation of Inner Ear Hair Cells. *Science* **284**, 1837–1841.
- Bertrand, N., Castro, D. S. and Guillemot, F.** (2002). Proneural genes and the specification of neural cell types. *Nat. Rev. Neurosci.* **3**, 517–530.

- Bok, J., Raft, S., Kong, K.-A., Koo, S. K., Dräger, U. C. and Wu, D. K.** (2011). Transient retinoic acid signaling confers anterior-posterior polarity to the inner ear. *Proceedings of the National Academy of Sciences* **108**, 161–166.
- Breau, M. A. and Schneider-Maunoury, S.** (2014). Mechanisms of cranial placode assembly. *Int. J. Dev. Biol.*
- Brown, A. S., Rakowiecki, S. M., Li, J. Y. H. and Epstein, D. J.** (2015). The cochlear sensory epithelium derives from Wnt responsive cells in the dorsomedial otic cup. *Developmental Biology* **399**, 177–187.
- Cai, T., Jen, H.-I., Kang, H., Klisch, T. J., Zoghbi, H. Y. and Groves, A. K.** (2015). Characterization of the transcriptome of nascent hair cells and identification of direct targets of the Atoh1 transcription factor. *Journal of Neuroscience* **35**, 5870–5883.
- Camarero, G., Leon, Y., Gorospe, I., De Pablo, F., Alsina, B., Giráldez, F. and Varela-Nieto, I.** (2003). Insulin-like growth factor 1 is required for survival of transit-amplifying neuroblasts and differentiation of otic neurons. *Developmental Biology* **262**, 242–253.
- Caron, S. J. C.** (2013). Brains Don't Play Dice--or Do They? *Science* **342**, 574–574.
- Caron, S. J. C., Prober, D., Choy, M. and Schier, A. F.** (2008). In vivo birthdating by BAPTISM reveals that trigeminal sensory neuron diversity depends on early neurogenesis. *Development* **135**, 3259–3269.
- Casper, B. M. and Mann, D. A.** (2007). The directional hearing abilities of two species of bamboo sharks. *J. Exp. Biol.* **210**, 505–511.
- Cepko, C.** (2014). Cepko_2015_nice. *Nature Publishing Group* **15**, 615–627.
- Chen, J. and Streit, A.** (2013). Induction of the inner ear: Stepwise specification of otic fate from multipotent progenitors. *Hearing Research* **297**, 3–12.
- Chen, P. and Segil, N.** (1999). p27(Kip1) links cell proliferation to morphogenesis in the developing organ of Corti. *Development* **126**, 1581–1590.
- Daudet, N. and Lewis, J.** (2005). Two contrasting roles for Notch activity in chick inner ear development: specification of prosensory patches and lateral inhibition of hair-cell differentiation. *Development* **132**, 541–551.
- Daudet, N., Ariza-McNaughton, L. and Lewis, J.** (2007). Notch signalling is needed to maintain, but not to initiate, the formation of prosensory patches in the chick inner ear. *Development* **134**, 2369–2378.
- Drobizhev, M., Makarov, N. S., Tillo, S. E., Hughes, T. E. and Rebane, A.** (2011). Two-photon absorption properties of fluorescent proteins. *Nat Meth* **8**, 393–399.

- Elliott, K. L., Houston, D. W., DeCook, R. and Fritzscht, B.** (2015). Ear manipulations reveal a critical period for survival and dendritic development at the single-cell level in Mauthner neurons. *Dev Neurobiol.*
- Fariñas, I., Jones, K. R., Tessarollo, L., Vigers, A. J., Huang, E., Kirstein, M., de Caprona, D. C., Coppola, V., Backus, C., Reichardt, L. F., et al.** (2001). Spatial shaping of cochlear innervation by temporally regulated neurotrophin expression. *Journal of Neuroscience* **21**, 6170–6180.
- Fekete, D. M. and Wu, D. K.** (2002). Revisiting cell fate specification in the inner ear. *Current Opinion in Neurobiology* **12**, 35–42.
- Flock, A., Bretscher, A. and Weber, K.** (1982). Immunohistochemical localization of several cytoskeletal proteins in inner ear sensory and supporting cells. *Hearing Research* **7**, 75–89.
- Freter, S., Muta, Y., Mak, S.-S., Rinkwitz, S. and Ladher, R. K.** (2008). Progressive restriction of otic fate: the role of FGF and Wnt in resolving inner ear potential. *Development* **135**, 3415–3424.
- Fritzscht, B. and Beisel, K. W.** (2001). Evolution and development of the vertebrate ear. *Brain Research Bulletin* **55**, 711–721.
- Fritzscht, B., Eberl, D. F. and Beisel, K. W.** (2010). The role of bHLH genes in ear development and evolution: revisiting a 10-year-old hypothesis. *Cell. Mol. Life Sci.* **67**, 3089–3099.
- Fritzscht, B., Matei, V. A., Nichols, D. H., Bermingham, N., Jones, K., Beisel, K. W. and Wang, V. Y.** (2005). Atoh1 null mice show directed afferent fiber growth to undifferentiated ear sensory epithelia followed by incomplete fiber retention. *Dev. Dyn.* **233**, 570–583.
- Gerety, S. S., Breau, M. A., Sasai, N., Xu, Q., Briscoe, J. and Wilkinson, D. G.** (2013). An inducible transgene expression system for zebrafish and chick. *Development* **140**, 2235–2243.
- Ghysen, A. and Dambly-Chaudière, C.** (1988). From DNA to form: the achaete-scute complex. *Genes & Development* **2**, 495–501.
- Giraldez_DevBiol_1998_Regionalized Organizing Activity of the Neural Tube Revealed by the Regulation of *lmx1* in the Otic Vesicle1** (1998).
Giraldez_DevBiol_1998_Regionalized Organizing Activity of the Neural Tube Revealed by the Regulation of *lmx1* in the Otic Vesicle1. 1–12.
- Gonzalez, D. M. and Medici, D.** (2014). Signaling mechanisms of the epithelial-mesenchymal transition. *Sci Signal* **7**, re8.
- Guillemot, F.** (2007). Cell fate specification in the mammalian telencephalon. *Progress in Neurobiology* **83**, 37–52.

- Guillemot, F.** (2007). Spatial and temporal specification of neural fates by transcription factor codes. *Development* **134**, 3771–3780.
- Haddon, C. and Lewis, J.** (1996). Early ear development in the embryo of the zebrafish, *Danio rerio*. *J. Comp. Neurol.* **365**, 113–128.
- Haddon, C., Jiang, Y. J., Smithers, L. and Lewis, J.** (1998). Delta-Notch signalling and the patterning of sensory cell differentiation in the zebrafish ear: evidence from the mind bomb mutant. *Development* **125**, 4637–4644.
- Hans, S., Irmscher, A. and Brand, M.** (2013). Zebrafish Foxi1 provides a neuronal ground state during inner ear induction preceding the Dlx3b/4b-regulated sensory lineage. *Development* **140**, 1936–1945.
- Harding, M. J. and Nechiporuk, A. V.** (2012). Fgfr-Ras-MAPK signaling is required for apical constriction via apical positioning of Rho-associated kinase during mechanosensory organ formation. *Development* **139**, 3130–3135.
- Hoijsman, E., Rubbini, D., Colombelli, J. and Alsina, B.** (2015). Mitotic cell rounding and epithelial thinning regulate lumen growth and shape. *Nature Communications* **6**, 7355.
- Hudspeth, A. J. and Corey, D. P.** (1977). Sensitivity, polarity, and conductance change in the response of vertebrate hair cells to controlled mechanical stimuli. *Proc. Natl. Acad. Sci. U.S.A.* **74**, 2407–2411.
- Jahan, I., Pan, N., Kersigo, J. and Fritzsche, B.** (2010). Neurod1 Suppresses Hair Cell Differentiation in Ear Ganglia and Regulates Hair Cell Subtype Development in the Cochlea. *PLoS ONE* **5**, e11661.
- Jarman, A. P., Grau, Y., Jan, L. Y. and Jan, Y. N.** (1993). atonal is a proneural gene that directs chordotonal organ formation in the *Drosophila* peripheral nervous system. *Cell* **73**, 1307–1321.
- Jones, J. M. and Warchol, M. E.** (2009). Expression of the Gata3 transcription factor in the acoustic ganglion of the developing avian inner ear. *J. Comp. Neurol.* **516**, 507–518.
- Kamaid, A., Neves, J. and Giráldez, F.** (2010). Id Gene Regulation and Function in the Prosensory Domains of the Chicken Inner Ear: A Link between Bmp Signaling and Atoh1. *Journal of Neuroscience* **30**, 11426–11434.
- Kani, S., Bae, Y.-K., Shimizu, T., Tanabe, K., Satou, C., Parsons, M. J., Scott, E., Higashijima, S.-I. and Hibi, M.** (2010). Proneural gene-linked neurogenesis in zebrafish cerebellum. *Developmental Biology* **343**, 1–17.
- Karis, A., Pata, I., van Doorninck, J. H., Grosveld, F., de Zeeuw, C. I., de Caprona, D. and Fritzsche, B.** (2001). Transcription factor GATA-3 alters pathway selection of olivocochlear neurons and affects morphogenesis of the ear. *J. Comp. Neurol.* **429**, 615–630.

- Kelley, M. W.** (2006). Regulation of cell fate in the sensory epithelia of the inner ear. *Nat. Rev. Neurosci.* **7**, 837–849.
- Kiernan, A. E., Pelling, A. L., Leung, K. K. H., Tang, A. S. P., Bell, D. M., Tease, C., Lovell-Badge, R., Steel, K. P. and Cheah, K. S. E.** (2005). Sox2 is required for sensory organ development in the mammalian inner ear. *Nature* **434**, 1031–1035.
- Kiernan, A. E., Xu, J. and Gridley, T.** (2006). The Notch ligand JAG1 is required for sensory progenitor development in the mammalian inner ear. *PLoS Genet* **2**, e4.
- Kim, W. Y., Fritsch, B., Serls, A., Bakel, L. A., Huang, E. J., Reichardt, L. F., Barth, D. S. and Lee, J. E.** (2001). NeuroD-null mice are deaf due to a severe loss of the inner ear sensory neurons during development. *Development* **128**, 417–426.
- Klisch, T. J., Xi, Y., Flora, A., Wang, L., Li, W. and Zoghbi, H. Y.** (2011). In vivo Atoh1 targetome reveals how a proneural transcription factor regulates cerebellar development. *Proceedings of the National Academy of Sciences* **108**, 3288–3293.
- Kogure, T., Kawano, H., Abe, Y. and Miyawaki, A.** (2008). Fluorescence imaging using a fluorescent protein with a large Stokes shift. *Methods* **45**, 223–226.
- Koundakjian, E. J., Appler, J. L. and Goodrich, L. V.** (2007). Auditory Neurons Make Stereotyped Wiring Decisions before Maturation of Their Targets. *Journal of Neuroscience* **27**, 14078–14088.
- Kwak, S.-J., Phillips, B. T., Heck, R. and Riley, B. B.** (2002). An expanded domain of fgf3 expression in the hindbrain of zebrafish valentino mutants results in mis-patterning of the otic vesicle. *Development* **129**, 5279–5287.
- Ladher, R. K., O'Neill, P. and Begbie, J.** (2010). From shared lineage to distinct functions: the development of the inner ear and epibranchial placodes. *Development* **137**, 1777–1785.
- Lai, H. C., Klisch, T. J., Roberts, R., Zoghbi, H. Y. and Johnson, J. E.** (2011). In Vivo Neuronal Subtype-Specific Targets of Atoh1 (Math1) in Dorsal Spinal Cord. *Journal of Neuroscience* **31**, 10859–10871.
- Lassiter, R. N. T., Stark, M. R., Zhao, T. and Zhou, C. J.** (2014). Signaling mechanisms controlling cranial placode neurogenesis and delamination. *Developmental Biology* **389**, 39–49.
- Lawoko-Kerali, G., Rivolta, M. N. and Holley, M.** (2001). Expression of the transcription factors GATA3 and Pax2 during development of the mammalian inner ear. *J. Comp. Neurol.* **442**, 378–391.
- Lawoko-Kerali, G., Rivolta, M. N., Lawlor, P., Cacciabue-Rivolta, D. I., Langton-Hewer, C., Hikke van Doorninck, J. and Holley, M. C.** (2004). GATA3 and NeuroD distinguish auditory and vestibular neurons during development of the mammalian inner ear. *Mechanisms of Development* **121**, 287–299.

- Lecaudey, V., Ulloa, E., Anselme, I., Stedman, A., Schneider-Maunoury, S. and Pujades, C.** (2007). Role of the hindbrain in patterning the otic vesicle: A study of the zebrafish *vhnf1* mutant. *Developmental Biology* **303**, 134–143.
- Levi-montalcini, R.** (1949). The development to the acoustico-vestibular centers in the chick embryo in the absence of the afferent root fibers and of descending fiber tracts. *J. Comp. Neurol.* **91**, 209–41– illust– incl 3 pl.
- Lewis, R. S. and Hudspeth, A. J.** (1983). Voltage- and ion-dependent conductances in solitary vertebrate hair cells. *Nature* **304**, 538–541.
- Liu, K., Rath, M., beta, D. R., Mueller, T., Skibbe, H., Drayer, B., Schmidt, T., Filippi, A., Nitschke, R., Brox, T., et al.** (2012a). ViBE-Z: a framework for 3D virtual colocalization analysis in zebrafish larval brains. *Nat Meth* 1–12.
- Liu, M., Pereira, F. A., Price, S. D. and Chu, M.** (2012b). Essential role of BETA2/NeuroD1 in development of the vestibular and auditory systems. *Genes & ...* 1–16.
- Ma, Q., Chen, Z., del Barco Barrantes, I., la Pompa, de, J. L. and Anderson, D. J.** (1998). *neurogenin1* is essential for the determination of neuronal precursors for proximal cranial sensory ganglia. *Neuron* **20**, 469–482.
- Ma, Q., Anderson, D. J. and Fritsch, B.** (2000). Neurogenin 1 Null Mutant Ears Develop Fewer, Morphologically Normal Hair Cells in Smaller Sensory Epithelia Devoid of Innervation. *JARO* **1**, 129–143.
- Ma, W.-R. and Zhang, J.** (2015). *Jag1b* is essential for patterning inner ear sensory cristae by regulating anterior morphogenetic tissue separation and preventing posterior cell death. *Development* **142**, 763–773.
- Maier, E. C. and Whitfield, T. T.** (2014). RA and FGF signalling are required in the zebrafish otic vesicle to pattern and maintain ventral otic identities. *PLoS Genet* **10**, e1004858.
- Maier, E. C., Saxena, A., Alsina, B., Bronner, M. E. and Whitfield, T. T.** (2014). Sensational placodes: neurogenesis in the otic and olfactory systems. *Developmental Biology* **389**, 50–67.
- Matei, V., Pauley, S., Kaing, S., Rowitch, D., Beisel, K. W., Morris, K., Feng, F., Jones, K., Lee, J. and Fritsch, B.** (2005). Smaller inner ear sensory epithelia in *Neurog1* null mice are related to earlier hair cell cycle exit. *Dev. Dyn.* **234**, 633–650.
- McCarroll, M. N., Lewis, Z. R., Culbertson, M. D., Martin, B. L., Kimelman, D. and Nechiporuk, A. V.** (2012). Graded levels of *Pax2a* and *Pax8* regulate cell differentiation during sensory placode formation. *Development* **139**, 2740–2750.

- Millimaki, B. B., Sweet, E. M. and Riley, B. B.** (2010). Sox2 is required for maintenance and regeneration, but not initial development, of hair cells in the zebrafish inner ear. *Developmental Biology* **338**, 262–269.
- Millimaki, B. B., Sweet, E. M., Dhasan, M. S. and Riley, B. B.** (2007). Zebrafish *atoh1* genes: classic proneural activity in the inner ear and regulation by Fgf and Notch. *Development* **134**, 295–305.
- Neves, J., Abelló, G., Petrovic, J. and Giraldez, F.** (2013a). Patterning and cell fate in the inner ear: a case for Notch in the chicken embryo. *Development, Growth & Differentiation* **55**, 96–112.
- Neves, J., Kamaid, A., Alsina, B. and Giraldez, F.** (2007). Differential expression of Sox2 and Sox3 in neuronal and sensory progenitors of the developing inner ear of the chick. *J. Comp. Neurol.* **503**, 487–500.
- Neves, J., Parada, C., Chamizo, M. and Giraldez, F.** (2011). Jagged 1 regulates the restriction of Sox2 expression in the developing chicken inner ear: a mechanism for sensory organ specification. *Development* **138**, 735–744.
- Neves, J., Uchikawa, M., Bigas, A. and Giraldez, F.** (2012). The Prosensory Function of Sox2 in the Chicken Inner Ear Relies on the Direct Regulation of Atoh1. *PLoS ONE* **7**, e30871.
- Neves, J., Vachkov, I. and Giraldez, F.** (2013b). Sox2 regulation of hair cell development: incoherence makes sense. *Hearing Research* **297**, 20–29.
- Ohyama, T., Basch, M. L., Mishina, Y., Lyons, K. M., Segil, N. and Groves, A. K.** (2010). BMP signaling is necessary for patterning the sensory and nonsensory regions of the developing mammalian cochlea. *Journal of Neuroscience* **30**, 15044–15051.
- Olivier, N., Luengo-Oroz, M. A., Duloquin, L., Faure, E., Savy, T., Veilleux, I., Solinas, X., Debarre, D., Bourguine, P., Santos, A., et al.** (2010). Cell Lineage Reconstruction of Early Zebrafish Embryos Using Label-Free Nonlinear Microscopy. *Science* **329**, 967–971.
- Pan, N., Jahan, I., Kersigo, J., Duncan, J. S., Kopecky, B. and Fritsch, B.** (2012). A Novel Atoh1 “Self-Terminating” Mouse Model Reveals the Necessity of Proper Atoh1 Level and Duration for Hair Cell Differentiation and Viability. *PLoS ONE* **7**, e30358.
- Pan, W., Jin, Y., Stanger, B. and Kiernan, A. E.** (2010). Notch signaling is required for the generation of hair cells and supporting cells in the mammalian inner ear. *Proceedings of the National Academy of Sciences* **107**, 15798–15803.
- Paridaen, J. T. M. L. and Huttner, W. B.** (2014). Neurogenesis during development of the vertebrate central nervous system. *EMBO Rep* **15**, 351–364.

- Park, S.-H., Yeo, S.-Y., Yoo, K.-W., Hong, S.-K., Lee, S., Rhee, M., Chitnis, A. B. and Kim, C.-H.** (2003). Zath3, a neural basic helix-loop-helix gene, regulates early neurogenesis in the zebrafish. *Biochemical and Biophysical Research Communications* **308**, 184–190.
- Patthey, C., Schlosser, G. and Shimeld, S. M.** (2014). The evolutionary history of vertebrate cranial placodes--I: cell type evolution. *Developmental Biology* **389**, 82–97.
- Petrovic, J., Gálvez, H., Neves, J., Abelló, G. and Giraldez, F.** (2014). Differential regulation of Hes/Hey genes during inner ear development. *Dev Neurobiol.*
- Pujades, C., Kamaid, A., Alsina, B. and Giraldez, F.** (2006). BMP-signaling regulates the generation of hair-cells. *Developmental Biology* **292**, 55–67.
- Purves, D., Augustine, G. J., Fitzpatrick, D. and Hall, W. C.** (2004). Neuroscience. 759.
- Radosevic, M., Robert-Moreno, A., Coolen, M., Bally-Cuif, L. and Alsina, B.** (2011). Her9 represses neurogenic fate downstream of Tbx1 and retinoic acid signaling in the inner ear. *Development* **138**, 397–408.
- Raft, S. and Groves, A. K.** (2015). Segregating neural and mechanosensory fates in the developing ear: patterning, signaling, and transcriptional control. *Cell Tissue Res* **359**, 315–332.
- Raft, S., Koundakjian, E. J., Quinones, H., Jayasena, C. S., Goodrich, L. V., Johnson, J. E., Segil, N. and Groves, A. K.** (2007). Cross-regulation of Ngn1 and Math1 coordinates the production of neurons and sensory hair cells during inner ear development. *Development* **134**, 4405–4415.
- Raft, S., Nowotschin, S., Liao, J. and Morrow, B. E.** (2004). Suppression of neural fate and control of inner ear morphogenesis by Tbx1. *Development* **131**, 1801–1812.
- Riccomagno, M. M., Martinu, L., Mulheisen, M., Wu, D. K. and Epstein, D. J.** (2002). Riccomango_GenDev_2002_Specification of the mammalian cochlea is dependent on Sonic hedgehog. *Genes & Development* **16**, 2365–2378.
- Riccomagno, M. M., Takada, S. and Epstein, D. J.** (2005). Wnt-dependent regulation of inner ear morphogenesis is balanced by the opposing and supporting roles of Shh. *Genes & Development* **19**, 1612–1623.
- Riley, B. B. and Grunwald, D. J.** (1996). A mutation in zebrafish affecting a localized cellular function required for normal ear development. *Developmental Biology* **179**, 427–435.
- Saade, M., Gutiérrez-Vallejo, I., Le Dréau, G., Rabadán, M. A., Miguez, D. G., Buceta, J. and Martí, E.** (2013). Sonic hedgehog signaling switches the mode of division in the developing nervous system. *Cell Rep* **4**, 492–503.

- Sai, X. and Ladher, R. K.** (2008). FGF signaling regulates cytoskeletal remodeling during epithelial morphogenesis. *Curr. Biol.* **18**, 976–981.
- Sapede, D. and Pujades, C.** (2010). Hedgehog Signaling Governs the Development of Otic Sensory Epithelium and Its Associated Innervation in Zebrafish. *Journal of Neuroscience* **30**, 3612–3623.
- Sapede, D., Dyballa, S. and Pujades, C.** (2012). Cell Lineage Analysis Reveals Three Different Progenitor Pools for Neurosensory Elements in the Otic Vesicle. *Journal of Neuroscience* **32**, 16424–16434.
- Sarrazin, A. F., Villablanca, E. J., Nuñez, V. A., Sandoval, P. C., Ghysen, A. and Allende, M. L.** (2006). Proneural gene requirement for hair cell differentiation in the zebrafish lateral line. *Developmental Biology* **295**, 534–545.
- Sato, T.** (2005). Clonal analysis of the relationships between mechanosensory cells and the neurons that innervate them in the chicken ear. *Development* **132**, 1687–1697.
- Schlosser, G. and Ahrens, K.** (2004). Molecular anatomy of placode development in *Xenopus laevis*. *Developmental Biology* **271**, 439–466.
- Schneider-Maunoury, S. and Pujades, C.** (2007). Hindbrain signals in otic regionalization: walk on the wild side. *Int. J. Dev. Biol.* **51**, 495–506.
- Siddiqui, S. A. and Cramer, K. S.** (2005). Differential expression of Eph receptors and ephrins in the cochlear ganglion and eighth cranial nerve of the chick embryo. *J. Comp. Neurol.* **482**, 309–319.
- Sinha, D. K., Neveu, P., Gagey, N., Aujard, I., Le Saux, T., Rampon, C., Gauron, C., Kawakami, K., Leucht, C., Bally-Cuif, L., et al.** (2012). Photoactivation of the CreERT2 Recombinase for Conditional Site-Specific Recombination with High Spatiotemporal Resolution. <http://dx.doi.org/10.1089/zeb.2009.0632> 1–7.
- Steventon, B., Mayor, R. and Streit, A.** (2012). Mutual repression between Gbx2 and Otx2 in sensory placodes reveals a general mechanism for ectodermal patterning. *Developmental Biology* **367**, 55–65.
- Sun, S.-K., Dee, C. T., Tripathi, V. B., Rengifo, A., Hirst, C. S. and Scotting, P. J.** (2007). Epibranchial and otic placodes are induced by a common Fgf signal, but their subsequent development is independent. *Developmental Biology* **303**, 675–686.
- Sweet, E. M., Vemaraju, S. and Riley, B. B.** (2011). Sox2 and Fgf interact with Atoh1 to promote sensory competence throughout the zebrafish inner ear. *Developmental Biology* **358**, 113–121.

- Vázquez-Echeverría, C., Domínguez-Frutos, E., Charnay, P., Schimmang, T. and Pujades, C.** (2008). Analysis of mouse kreisler mutants reveals new roles of hindbrain-derived signals in the establishment of the otic neurogenic domain. *Developmental Biology* **322**, 167–178.
- Vemaraju, S., Kantarci, H., Padanad, M. S. and Riley, B. B.** (2012). A spatial and temporal gradient of Fgf differentially regulates distinct stages of neural development in the zebrafish inner ear. *PLoS Genet* **8**, e1003068.
- Whitfield, T. T., Riley, B. B., Chiang, M.-Y. and Phillips, B.** (2002). Development of the zebrafish inner ear. *Dev. Dyn.* **223**, 427–458.
- Witte, S., Negrean, A., Lodder, J. C., de Kock, C. P. J., Silva, G. T., Mansvelder, H. D. and Groot, M. L.** (2011). Label-free live brain imaging and targeted patching with third-harmonic generation microscopy. *Proceedings of the ...* **108**, 5970–5975.
- Xiong, F., Tentner, A. R., Huang, P., Gelas, A., Mosaliganti, K. R., Souhait, L., Rannou, N., Swinburne, I. A., Obholzer, N. D., Cowgill, P. D., et al.** (2013). Specified neural progenitors sort to form sharp domains after noisy Shh signaling. *Cell* **153**, 550–561.
- Zanazzi, G. and Matthews, G.** (2009). The Molecular Architecture of Ribbon Presynaptic Terminals. *Mol Neurobiol* **39**, 130–148.
- Zecca, A., Dyballa, S., Voltes, A., Bradley, R. and Pujades, C.** (2015). The Order and Place of Neuronal Differentiation Establish the Topography of Sensory Projections and the Entry Points within the Hindbrain. *Journal of Neuroscience* **35**, 7475–7486.
- Zecchin, E., Conigliaro, A., Tiso, N., Argenton, F. and Bortolussi, M.** (2005). Expression analysis of jagged genes in zebrafish embryos. *Dev. Dyn.* **233**, 638–645.
- Zipfel, W. R., Williams, R. M. and Webb, W. W.** (2003). Nonlinear magic: multiphoton microscopy in the biosciences. *Nat Biotech* **21**, 1369–1377.